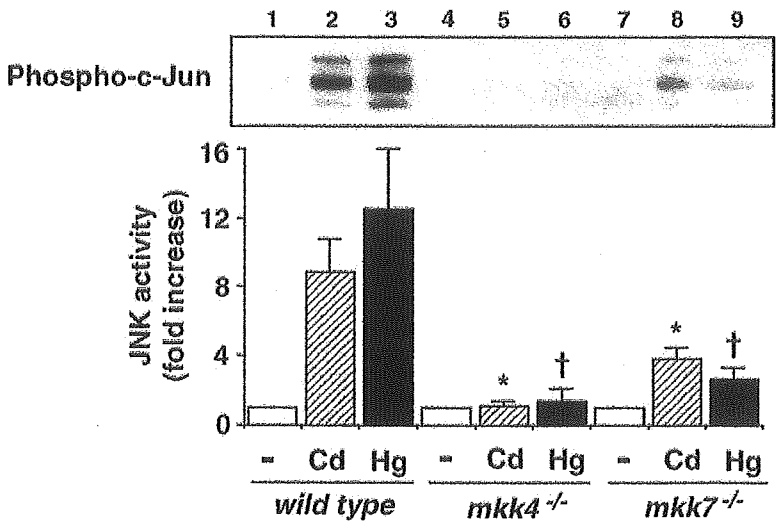

Fig. 4. Effects of $CdCl_2$ or $HgCl_2$ treatment on the activity of JNK in wild-type, *mkk4*$^{-/-}$ and *mkk7*$^{-/-}$ ES cells. Wild-type, *mkk4*$^{-/-}$ and *mkk7*$^{-/-}$ ES cells were incubated with serum-free medium (lanes 1, 4, and 7), 20 μM $CdCl_2$ (lanes 2, 5, and 8) or 20 μM $HgCl_2$ (lanes 3, 6, and 9) for 1 h, and cell lysates were used for in vitro kinase reaction with GST-c-Jun (1–89) as substrate. Phosphorylation of GST-c-Jun was analyzed with immunoblotting using anti-phospho-c-Jun antibody. Results shown are representative immunoblot and densitometric analysis of phosphorylated c-Jun. Each value was expressed as the fold increase with respect to the corresponding control (without metal treatments). Each column and bar represent the mean ± S.D. of four independent experiments. $^{*}P < 0.01$ compared to wild-type ES cells treated with $CdCl_2$, $^{\dagger}P < 0.01$ compared to wild-type ES cells treated with $HgCl_2$.

these mutated cell lines. These findings suggest that the full activation of JNK by toxic metal exposure requires both MKK4 and MKK7, and these upstream kinases might contribute differentially in JNK activation between ES cells exposed to $CdCl_2$ and $HgCl_2$. $CdCl_2$-induced JNK activation seems to depend on MKK4 more extensively than MKK7.

In contrast, previous studies using cells transfected with dominant-negative form of MKK4 or MKK7 showed that cadmium might activate JNK through MKK7, but not MKK4. Transfection with MKK4 mutant elevated $CdCl_2$ (80 μM, 3 h exposure) -induced JNK activation 1.9-fold in human non-small-cell lung carcinoma cells, while expression of MKK7 mutant reduced JNK activity by 35% (Chuang and Yang, 2001). However, expression of MKK7 mutant failed to suppress JNK activity in the same cells treated with a higher concentration of $CdCl_2$ (130 μM) (Chuang et al., 2000). In rat mesangial cells, $CdCl_2$ (10 μM, 8 h exposure) -induced JNK activation was suppressed by 53% when transfected with MKK7 mutant, but not changed by expression of MKK4 mutant (Ding and Templeton, 2000). On the other hand, it has been reported that treatment with $CdCl_2$ induced the phosphorylation of MKK4 in Rat-1 fibroblasts (Iordanov and Magun, 1999), and we also found the phosphorylation of MKK4 on Thr^{261} in wild-type ES cells following exposure to $CdCl_2$ or $HgCl_2$ (data not shown). Thus, MKK4 could be activated by upstream kinase (i.e., MAPK kinase kinase) in response to $CdCl_2$ or $HgCl_2$ exposure, and disruption of the *mkk4* gene abolished toxic metal-induced JNK activation almost completely in ES cells. While the precise functions of MKK4 and MKK7 in cells exposed to toxic metal are still not clear, these MAPK kinases might play a different role in JNK activation depending on the cell type and the experimental condition of exposure. With respect to mkk4$^{-/-}$ and *mkk7*$^{-/-}$ ES cells exposed to $CdCl_2$ or $HgCl_2$, the roles of splice variants and the effects of JNK (p46) expression remain to be examined.

In summary, as has been shown in various stress-induced JNK activation (Kishimoto et al., 2003; Wada et al., 2001), both MKK4 and MKK7 were required for the full activation of JNK in mouse ES cells exposed to $CdCl_2$ or $HgCl_2$. The *mkk4*$^{-/-}$ and *mkk7*$^{-/-}$ ES cells seem to be useful to analyze functions and signaling pathway of JNK activation induced by environmental stresses including toxic metals.

Acknowledgements

We thank Takeo Okuno for technical help. This work was supported in part by Grant-in-Aid for Scientific Research (KAKENHI: 14570313 and 14570315) from the Ministry of Education, Culture, Sports, Science and Technology (MEXT), Japan.

References

Chang, L., Karin, M., 2001. Mammalian MAP kinase signalling cascades. Nature 410, 37–40.

Chuang, S.-M., Yang, J.-L., 2001. Comparison of roles of three mitogen-activated protein kinases induced by chromium (VI) and cadmium in non-small-cell lung carcinoma cells. Mol. Cell. Biochem. 222, 85–95.

Chuang, S.-M., Wang, I.-C., Yang, J.-L., 2000. Roles of JNK, p38 and ERK mitogen-activated protein kinases in the growth inhibition and apoptosis induced by cadmium. Carcinogenesis 21, 1423–1432.

Cobb, M.H., Goldsmith, E.J., 1995. How MAP kinases are regulated. J. Biol. Chem. 270, 14843–14846.

Ding, W., Templeton, D.M., 2000. Stress-activated protein kinase-dependent induction of c-*fos* by Cd^{2+} is mediated by MKK7. Biochem. Biophys. Res. Commun. 273, 718–722.

Iordanov, M.S., Magun, B.E., 1999. Different mechanisms of c-Jun NH_2-terminal kinase-1 (JNK1) activation by ultraviolet-B radiation and by oxidative stressors. J. Biol. Chem. 274, 25801–25806.

Kishimoto, H., Nakagawa, K., Watanabe, T., Kitagawa, D., Momose, H., Seo, J., Nishitai, G., Shimizu, N., Ohata, S., Tanemura, S., Asaka, S., Goto, T., Fukushi, H., Yoshida, H., Suzuki, A., Sasaki, T., Wada, T., Penninger, J.M., Nishina, H., Katada, T., 2003. Different properties of SEK1 and MKK7 in dual phosphorylation of stress-induced activated protein kinase SAPK/JNK in embryonic stem cells. J. Biol. Chem. 278, 16595–16601.

Kyriakis, J.M., Avruch, J., 1996. Sounding the alarm: protein kinase cascades activated by stress and inflammation. J. Biol. Chem. 271, 24313–24316.

Lawler, S., Fleming, Y., Goedert, M., Cohen, P., 1998. Synergistic activation of SAPK1/JNK1 by two MAP kinase kinases in vitro. Curr. Biol. 8, 1387–1390.

Matsuoka, M., Igisu, H., 1998. Activation of c-Jun NH_2-terminal kinase (JNK/SAPK) in LLC-PK_1 cells by cadmium. Biochem. Biophys. Res. Commun. 251, 527–532.

Matsuoka, M., Igisu, H., 2002. Effects of heavy metals on mitogen-activated protein kinase pathways. Environ. Health Prev. Med. 6, 210–217.

Matsuoka, M., Wispriyono, B., Iryo, Y., Igisu, H., 2000. Mercury chloride activates c-Jun N-terminal kinase and induces c-*jun* expression in LLC-PK_1 cells. Toxicol. Sci. 53, 361–368.

Nishina, H., Fischer, K.D., Radvanyi, L., Shahinian, A., Hakem, R., Rubie, E.A., Bernstein, A., Mak, T.W., Woodgett, J.R., Penninger, J.M., 1997. Stress-signalling kinase Sek1 protects thymocytes from apoptosis mediated by CD95 and CD3. Nature 385, 350–353.

Robinson, M.J., Cobb, M.H., 1997. Mitogen-activated protein kinase pathways. Curr. Opin. Cell Biol. 9, 180–186.

Wada, T., Nakagawa, K., Watanabe, T., Nishitai, G., Seo, J., Kishimoto, H., Kitagawa, D., Sasaki, T., Penninger, J.M., Nishina, H., Katada, T., 2001. Impaired synergistic activation of stress-activated protein kinase SAPK/JNK in mouse embryonic stem cells lacking SEK1/MKK4: different contribution of SEK2/MKK7 isoforms to the synergistic activation. J. Biol. Chem. 276, 30892–30897.

Weston, C.R., Davis, R.J., 2002. The JNK signal transduction pathway. Curr. Opin. Genet. Dev. 12, 14–21.

Yu, Z., Matsuoka, M., Wispriyono, B., Iryo, Y., Igisu, H., 2000. Activation of mitogen-activated protein kinases by tributyltin in CCRF-CEM cells: role of intracellular Ca^{2+}. Toxicol. Appl. Pharmacol. 168, 200–207.

ELSEVIER

Mechanisms of Development 121 (2004) 647–658

www.elsevier.com/locate/modo

Research paper

A systematic genome-wide screen for mutations affecting organogenesis in Medaka, *Oryzias latipes*

Makoto Furutani-Seiki[a,*], Takao Sasado[a], Chikako Morinaga[a], Hiroshi Suwa[a], Katsutoshi Niwa[a], Hiroki Yoda[b], Tomonori Deguchi[b], Yukihiro Hirose[c], Akihito Yasuoka[d], Thorsten Henrich[a], Tomomi Watanabe[e], Norimasa Iwanami[f], Daiju Kitagawa[e], Kota Saito[e], Satoshi Asaka[e], Masakazu Osakada[g], Sanae Kunimatsu[f], Akihiro Momoi[b], Harun Elmasri[h], Christoph Winkler[h], Mirana Ramialison[a], Felix Loosli[i], Rebecca Quiring[i], Matthias Carl[i], Clemens Grabher[i], Sylke Winkler[i], Filippo Del Bene[i], Ai Shinomiya[j], Yasuko Kota[a], Toshiyuki Yamanaka[a], Yasuko Okamoto[a], Katsuhito Takahashi[g], Takeshi Todo[k], Keiko Abe[d], Yousuke Takahama[f], Minoru Tanaka[l], Hiroshi Mitani[m], Toshiaki Katada[e], Hiroshi Nishina[e], Noboru Nakajima[a], Joachim Wittbrodt[i], Hisato Kondoh[a,b,*]

[a]*Japan Science and Technology Corporation, Kondoh Differentiation Signaling Project, Kawaaracho 14, Yoshida, Sakyoku, Kyoto 606-8305, Japan*
[b]*Graduate School of Frontier Biosciences, Osaka University, Osaka 565-0871, Japan*
[c]*Graduate School of Biostudies, Kyoto University, Kyoto 606-8502, Japan*
[d]*Graduate School of Agricultural and Life Sciences, The University of Tokyo, Tokyo 113-0033, Japan*
[e]*Department of Physiological Chemistry, Graduate School of Pharmaceutical Sciences, The University of Tokyo, Tokyo 113-0033, Japan*
[f]*Division of Experimental Immunology, Institute for Genome Research, The University of Tokushima, Tokushima 770-8503, Japan*
[g]*Department of Molecular Medicine and Pathophysiology, Research Institute, Osaka Medical Center for Cancer and Cardiovascular Diseases, Osaka 537-8511, Japan*
[h]*Physiological Chemistry I, Biocenter, University of Wuerzburg, D-97074 Wuerzburg, Germany*
[i]*Developmental Biology Programme, EMBL Heidelberg, D-69117 Heidelberg, Germany*
[j]*Department of Environmental Science, Faculty of Science, Niigata University, Niigata 950-2181, Japan*
[k]*Radiation Biology Center, Kyoto University, Kyoto 606-8501, Japan*
[l]*Division of Biological Sciences, Graduate School of Sciences, Hokkaido University, Hokkaido 060-0808, Japan*
[m]*Department of Integrated Biosciences, Graduate School of Frontier Sciences, The University of Tokyo, Chiba 277-8562, Japan*

Received 1 February 2004; received in revised form 22 March 2004; accepted 21 April 2004

Abstract

A large-scale mutagenesis screen was performed in Medaka to identify genes acting in diverse developmental processes. Mutations were identified in homozygous F3 progeny derived from ENU-treated founder males. In addition to the morphological inspection of live embryos, other approaches were used to detect abnormalities in organogenesis and in specific cellular processes, including germ cell migration, nerve tract formation, sensory organ differentiation and DNA repair. Among 2031 embryonic lethal mutations identified, 312 causing defects in organogenesis were selected for further analyses. From these, 126 mutations were characterized genetically and assigned to 105 genes. The similarity of the development of Medaka and zebrafish facilitated the comparison of mutant phenotypes, which indicated that many mutations in Medaka cause unique phenotypes so far unrecorded in zebrafish. Even when mutations of the two fish species cause a similar phenotype such as *one-eyed-pinhead* or *parachute*, more genes were found in Medaka than in zebrafish that produced the same phenotype when mutated. These observations suggest that many Medaka mutants represent new genes and, therefore, are important complements to the collection of zebrafish mutants that have proven so valuable for exploring genomic function in development.

Keywords: Medaka; Mutants; Interspecies difference; ENU mutagenesis; Vertebrate organogenesis; Kyoto screen

* Corresponding authors. Tel.: +81-75-771-9362; fax: +81-75-771-8281.
E-mail addresses: furutaniseiki@dsp.jst.go.jp (M. Furutani-Seiki), j61056@hpc.cmc.osaka-u.ac.jp (H. Kondoh).

0925-4773/$ - see front matter © 2004 Published by Elsevier Ireland Ltd.
doi:10.1016/j.mod.2004.04.016

1. Introduction

Mutants serve as an important entry point to the understanding of gene function. In particular, systematic screening for mutations among a mutagenized population of model organisms has been a powerful approach to identifying genes and their functions involved in specific cellular processes. The assignment of individual genes responsible for mutations has been greatly facilitated by recent advances in genomic research (e.g. physical maps and whole-genome sequencing). This approach has been particularly useful in revealing the ontogenetic process, and was successfully applied to invertebrate animals and plants, such as *Drosophila melanogaster*, *Caenorhabditis elegans*, and *Arabidopsis thaliana* (Nüsslein-Volhard and Wieschaus, 1980; Brenner, 1974; Mayer, 1991).

Among vertebrates, small fish are suitable for mutational investigations, for their ease of rearing in a relatively compact space, reasonably short generation time and, in particular, the translucent embryos they produce. In many species, embryos develop outside the mothers' body rendering them easy to inspect visually and to manipulate their tissues and cells (refer to Kimmel, 1989). One such fish is the zebrafish, *Danio rerio*; the accomplishment of large-scale mutagenesis screens (Haffter et al., 1996; Driever et al., 1996) and use of mutants to study developmental processes carried out in the past two decades have established the zebrafish as the premier vertebrate for unbiased analyses of genomic functions in development.

However, the use of a single species for mutagenesis screening will not be sufficient to uncover all gene functions, partly because of functional overlap among related genes, which is a common feature of vertebrates. This problem may be alleviated by the use of a second fish species where usage of genes may vary subtly from zebrafish. We therefore adopted Medaka as another fish species for large-scale identification and recovery of mutations. Medaka, *Oryzias latipes*, has been used as an experimental model animal since the 1920s (Aida, 1921). Sex chromosome-dependent sex determination (Aida, 1921), demonstration of hormone-induced sex reversal (Yamamoto, 1965) and identification of the sex determining gene DMY (Matsuda et al., 2002; Nanda et al., 2002) made this fish species a good model to study the mechanisms of sexual differentiation. Genetic tools have been generated including established inbred strains (Hyodo-Taguchi et al., 1983), a fine-scale genetic map derived from polymorphic markers (Naruse et al., 2000) and quantitative trait loci (Ishikawa, 2000). Medaka has a small genome size (one-half of that of zebrafish and only twice that of Fugu) and is phylogenically distant from zebrafish, diverging about 110 million years ago (Wittbrodt et al., 2002), making it useful for comparisons of conserved and divergent gene functions in teleost evolution (Ohno, 1970; Amores et al., 1998).

Small-scale pilot screens for mutations affecting the development of the eyes and nervous system (Loosli, et al., 2000; Ishikawa, 2000) suggested a significantly different spectrum of mutant phenotypes from those described for zebrafish and provided encouragement for expanded mutagenesis screening using Medaka.

In this overview paper, we summarize the results of a large-scale systematic screen for mutations in Medaka. The major focus of this mutant screen was on embryonic pattern formation and organogenesis. In addition to morphological criteria, a variety of labeling techniques were used to detect abnormalities in specific cellular features or cell behaviors. The Kyoto collection of Medaka mutants will complement and extend analyses on zebrafish and mouse mutants (Hrabe de Angelis et al., 2000; Nolan et al., 2000) and expand our understanding of general mechanisms underlying organogenesis.

2. Results

2.1. Overall design of mutagenesis screen

We carried out a large-scale mutagenesis screen to detect mutations that produce defects ranging from early body patterning to cellular differentiation and organ formation. In addition to morphological criteria, various screening procedures were used to detect more subtle abnormalities in specific structures or functional processes. Germ line cells, thymocytes, optic, cranial and lateral line nerves, and optic tectal projections of retinal ganglion cell (RGC) axons were visualized by in situ hybridization, immunostaining or fluorescent dye injection in fixed embryos. In addition, the potential for DNA repair and bilirubin and lipid metabolism associated with liver function were examined.

An essential step in a large-scale mutagenesis screen is to start with a wild-type strain suitable for identifying zygotic, recessive mutations. After brother–sister mating from the Cab strain (Wittbrodt et al., 2002) for more than nine generations, a substrain (Kyoto-Cab strain) was selected for high fecundity and a low background of abnormal embryonic development. A three-generation in-crossing scheme was used to generate F3 embryos homozygous for mutations induced in founder males (Fig. 1).

To introduce mutations into the germ line, male founder adult fish were treated with ENU (*N*-ethyl-*N*-nitrosourea) (Shima and Shimada, 1988), which has been used for mutagenesis in zebrafish (Mullins et al., 1994; Solnica-Krezel et al., 1994) and mice (Russell and Montgomery, 1982). ENU is known to introduce point mutations very efficiently and relatively randomly in spermatogonia (Russell and Montgomery, 1982). Crossing ENU-treated founder males with albino mutant females (specific locus test) indicated the efficiency of mutagenesis ranged from 1/196 to 1/726 under the conditions employed (refer to Section 4).

We raised ca. 1300 F2 families, and used 1137 F2 families to produce the potentially homozygous F3 embryos

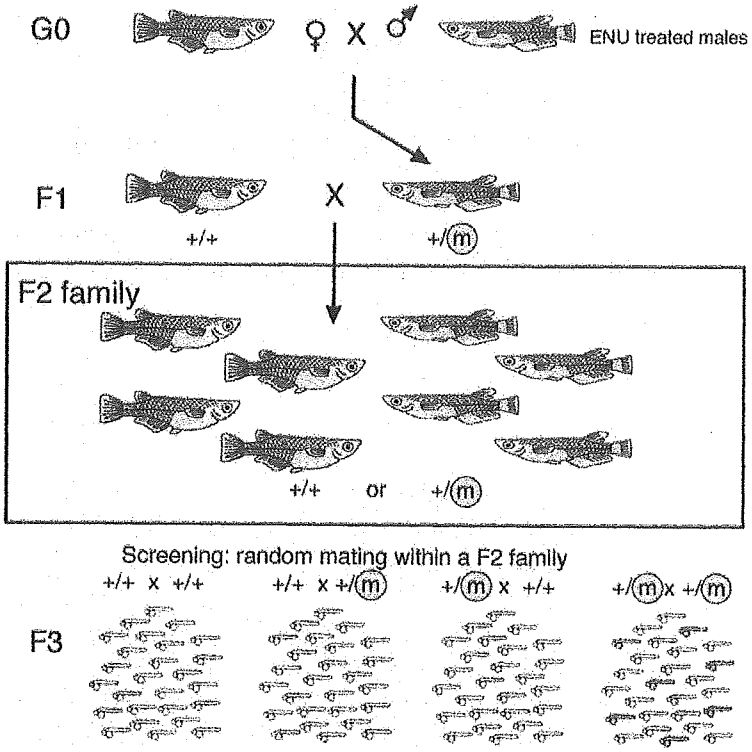

Fig. 1. A scheme of breeding of mutagenized fish population to identify recessive mutations (Adopted from Haffter et al., 1996, with modification). Males 4 weeks after treatment with ENU were mated with wild-type females to produce F1 progeny, which are heterozygous carriers of mutations derived from the mutagenized paternal genome. Many pairs of F1 fish were mated to generate F2 families, each consisting of about 60 fish derived from a single pair. A mutation designated as **m** harbored in an F1 parent is transmitted to one-half of the F2 families. Random brother–sister mating within an F2 family is expected to produce homozygotes of the mutation at a frequency of 1/4, assuming that the Mendelian ratio applies: When both F2 parents are heterozygous for mutation **m**, one-fourth of their F3 progeny will be homozygous for **m** and exhibit the mutant phenotype (shown on the right side).

bearing mutations. Of the more than 6700 F2 pairs mated, 6088 intercross pairs successfully produced progeny, and 24,887 clutches (a set of eggs produced per mating) were used for mutant screening. Nearly 260,000 F3 embryos were inspected during the screen. In total, 1588 mutagenized haploid genomes were screened for recessive mutations.

2.2. *Detection of mutant phenotypes*

Screening for morphological abnormalities in live embryos was performed at three stages of development, namely st. 19–21 (27–34 hpf, hours post-fertilization), st. 25–27 (50–58 hpf) and st. 32–35 (4 dpf, days post-fertilization) (Fig. 2). The earliest stage was chosen for identifying defects in early embryonic patterning, including gastrulation, dorso-ventral polarity, body axis formation, and early tissue degeneration. Screening at the second time point focused on the rudiments of organs, such as the eye vesicles, brain, heart primordium, otic vesicles, somites and notochord. At the third time point, abnormalities in organ morphogenesis were detected by screening the olfactory bulbs, brain ventricles, otic vesicles, liver, heart, vasculature, and pectoral fin buds. Special attention was paid to morphological abnormalities accompanied by cell degeneration, since specific patterning defects can produce localized cell degeneration at later stages (Furutani-Seiki et al., 1996).

While zebrafish lay about 100 eggs once in 1–2 weeks, Medaka spawns 10–40 eggs daily. We thus collected embryos from each pair for five consecutive days per week over two-week period, and used these different clutches of embryos in multiple assays. This feature of the Medaka system enabled simultaneous inspection of different clutches of embryos from the same parental pair at staggered developmental stages. Simultaneous observation of embryos at different ages but derived from the same parents also provided confirmation that abnormalities were genetic rather than the result of compromised egg quality.

Phenotypes affecting specific cell types were assessed by labeling of whole-mount specimens of fixed embryos using tissue-specific riboprobes (Fig. 3). In situ hybridization with a vasa probe allowed the visualization of primordial germ cells (Fig. 3A,A′) and differentiated germ cells (Fig. 3B,B″) at st. 26 (59 hpf) and 15 dpf, respectively (Shinomiya et al.,

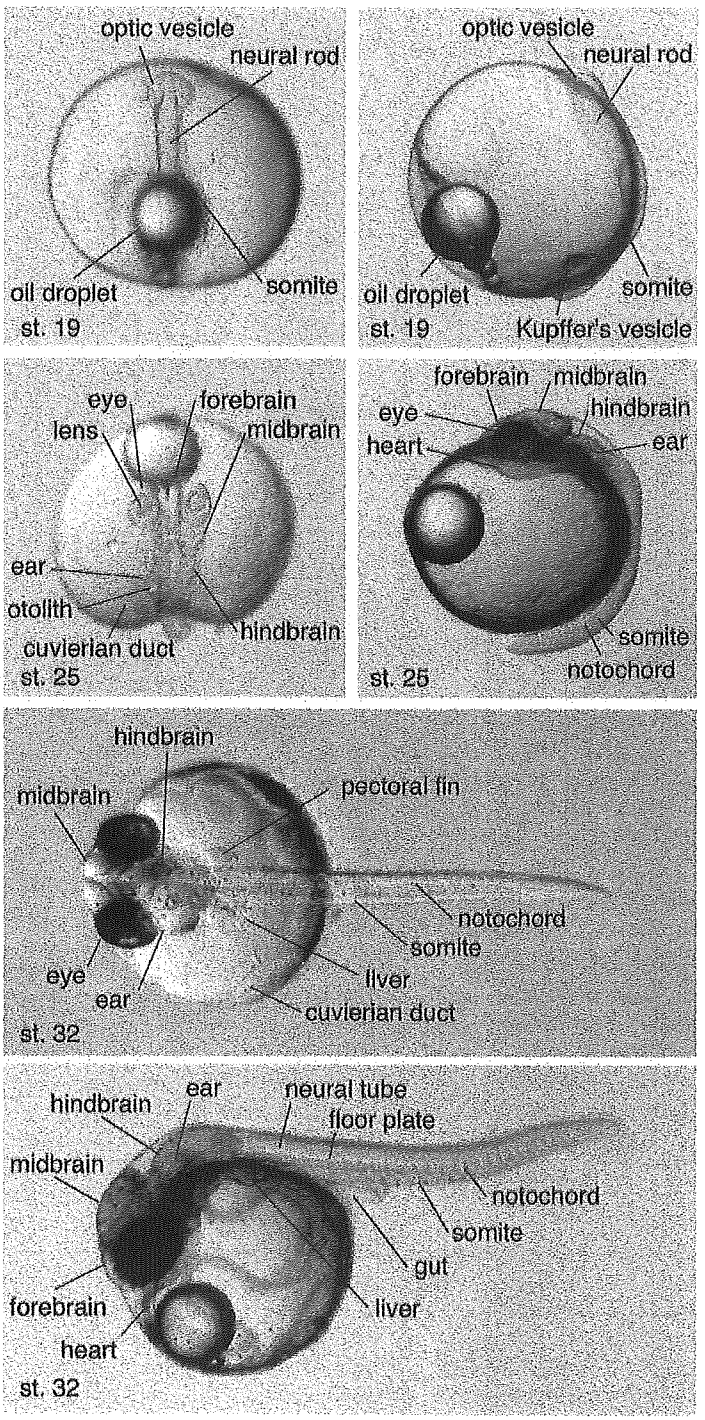

Fig. 2. Images of live Medaka embryos at three developmental stages when mutants were screened by morphological criteria. Visible structures in live embryos are marked.

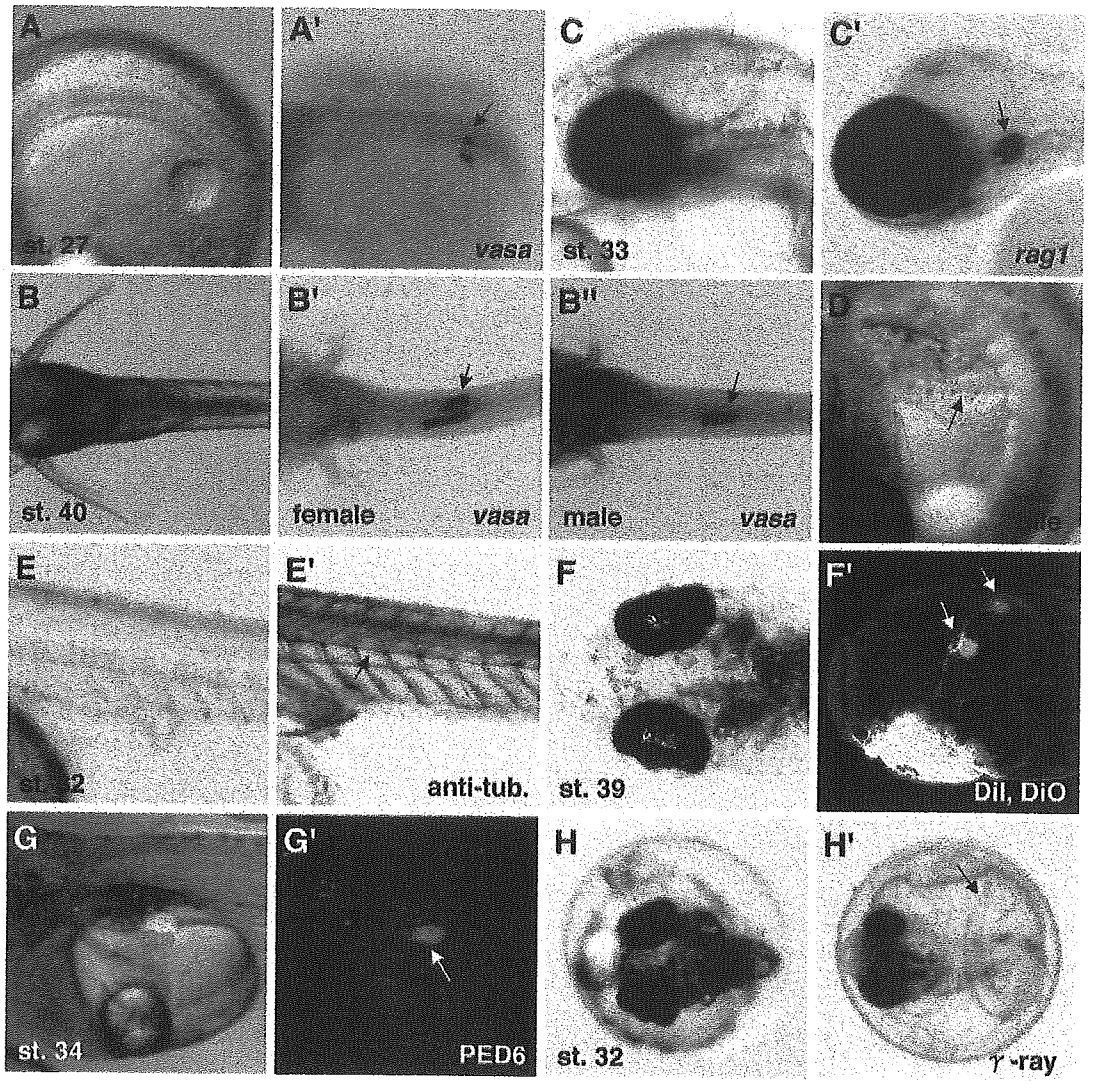

Fig. 3. Various assays employed in screening of Medaka mutants. (A, A′) St. 27 embryos, (A) live and (A′) *vasa* in situ hybridization detecting PGCs (arrow) colonizing in the gonad area of the trunk. (B. B′, B″) Early larva at st. 40, (B) live and (B′, B″) *vasa* in situ hybridization of st. 40 larvae, showing gonads containing abundant *vasa*-positive germ cells (arrow). A female larva (B′) usually has a larger right gonad than a male (B″). (C, C′) Anterior part of st. 33 embryos, (C) live and (C′) *rag1* in situ hybridization showing the location of thymus (arrow). (D) St. 34 live embryo, metabolism of hemoglobin to bilirubin was monitored by the color of bile in the gall bladder (arrow). (E, E′) Posterior part of st. 32 embryos, (E) live embryo and (E′) posterior lateral line nerves (arrow) visualized by immunostaining of acetylated tubulin and HNK-1 epitope. (F, F′) St. 39 larvae that have just hatched, (F) a live larva, (F′) labeling RGC axons projecting to foci of the contralateral tectum (arrows) by injecting lipophilic fluorescent dyes, DiI and DiO in the retina at fixed retinal positions. (G, G′) A live embryo at st. 34 loaded with PED6 and showing accumulation of its fluorescent metabolites in the gall bladder, under bright field illumination (G) and in fluorescent image (arrow) (G′). (H, H′) Effect of γ-ray irradiation on embryogenesis. (H) A wild-type embryo with a chorion at st. 32 recovered from irradiation with a semi-lethal dose of γ-ray at st.24. (H′) A homozygous γ-ray-sensitive mutant (*ric1*) showing a curled tail (arrow), characteristic indication of γ-ray sensitivity. (A, A′) semi-lateral view; (B-B″) ventral view; (C, C′, D, E, E′, G, G′) lateral view; (F, F′, H, H′) dorsal view.

2000). The *rag1* probe was used to detect thymocytes in st. 32 embryos (Fig. 3C,C′). Immunostaining using a mixture of anti-acetylated tubulin and HNK1 antibodies was performed to detect axons forming cranial and lateral line nerves at st. 32 (Fig. 3E,E′). The topographic projection of axons from RGCs to the optic tectum was visualized by injecting DiI and DiO at the ventrotemporal and dorsonasal positions, respectively, of retinas, as previously described in a screen for zebrafish retinotectal mutants (Fig. 3F,F′) (Baier et al., 1996).

Liver-associated physiological activity involving bile and lipid metabolism was scored by bile color (Fig. 3D) and the accumulation of a fluorescent metabolite of PED6, a phospholipase A_2 substrate (Farber et al., 2001), in the gall

Table 1
Numerical record of mutations identified in the Kyoto Medaka screen

Mutants	Number	Percentage
Total lethal mutations identified[a]	2031	100
F3 progeny raised	372	18
Newly discovered mutations in the F3 progeny	21	1.0
Mutations confirmed and recovered	312	15
Mutations not confirmed in the F3 progeny	39	1.9
Mutations lost during rearing F3 progeny	45	2.2
Mutations already assigned to genes	126	6.2
Mutations in the process of gene assignment	186	9.1

[a] Confirmed by repeated occurrences of the same phenotype in different clutches from the same parental pair.

bladder in living embryos (Fig. 3G,G′). DNA repair activity during embryogenesis was tested by examining recovery after exposure of developing embryos to a sublethal dose of γ-ray radiation (Fig. 3H,H′).

Together, using all of the screening methods, a total of 2031 embryonic lethal mutations were identified (Table 1). As Medaka embryos hatch at 9 dpf at 28 °C, mutant embryos that failed to hatch by this time were defined as carrying embryonic lethal mutations. Among these mutations, we selected 372 for further analyses on the basis of their specific phenotypes. F2 parents carrying the mutations of interest were outcrossed to wild-type fish and the F3 progeny raised and used for reidentification and recovery of mutations. The remaining mutations caused (1) non-specific general abnormalities, such as overall degeneration, retardation and edema as reported previously in zebrafish (Mullins et al., 1994; Solnica-Krezel et al., 1994) or (2) more specific phenotypes that were also accompanied by generalized retardation or degeneration. From the F3 generation, a total of 312 mutations were recovered and subjected to more detailed characterization.

2.3. Mutant classification and complementation analysis

Mutations recovered from the F3 generation were grouped into several classes according to the phenotype of homozygous mutants (Table 2). Within a class, heterozygous carriers of independently isolated mutations were intercrossed to test for genetic complementation. Complementation testing was completed for 126 mutations, and indicated that these mutations define 105 distinct genetic loci.

Table 2
Summary of identified gene according to the affected tissues

Tissues affected by the mutations	Genomes screened	Genes (mutations)
Forebrain	1588	25 (33)
Primordial germ cells	450	10 (12)
Gonad	428	13 (16)
Lateral line	432	4 (4)
Liver	162	19 (22)
Thymus	502	13 (15)
Eye	529	22 (25)
Retino-tectal pathfinding	184	5 (7)
Somite	1588	9 (12)
γ-Ray sensitivity	780	3 (3)

2.4. Mutant phenotypes

2.4.1. Forebrain mutants

Formation of the forebrain was affected in 33 mutants of 25 genes (Kitagawa et al., 2004). The mutations were grouped into two major phenotypic classes: Group 1 included mutations in 11 genes that resulted in a reduced telencephalon and Group 2 mutations in 14 genes produced abnormal morphology of the telencephalon without significantly affecting its size. In zebrafish, the development of the telencephalon is affected in *knollnase* (*kas*), *masterblind* (*mbl*) and *silberblick* (*slb*) embryos (Heisenberg et al., 1996), and mutants associated with midline defects resulting in cyclopia or a curly tail down phenotype (Brand et al., 1996). Mutations in Medaka affecting forebrain formation appear distinct from those in zebrafish as judged by their morphology (Fig. 4), although a careful comparison of Medaka and zebrafish mutant phenotypes using specific markers is necessary to confirm this observation. As noted above, tissue degeneration

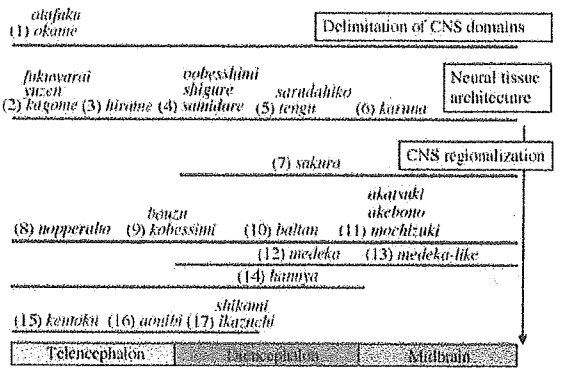

Fig. 4. Schematic presentation of Medaka mutations affecting anterior CNS and possible correspondence with the phenotypes of zebrafish mutants. Medaka mutants are roughly classified into 17 groups according to their phenotype, and the regions of CNS affected by the group of mutations are indicated by horizontal lines. Possible defect at cellular and tissue levels featuring the phenotype is indicated in the square. Medaka mutants displaying phenotypes resembling those of zebrafish mutations are indicated in red. Group 4 mutants of three genes exhibit a phenotype similar to that of the *parachute* zebrafish mutant. Group 8 mutants of one gene show the phenotypes analogous to those of *masterblind* and *headless* mutants. Group 11 mutants of three genes display the phenotype resembling to those of *one-eyed-pinhead* zebrafish mutants. Remaining mutations, possibly representing unique phenotypes of Medaka mutations, are indicated in blue. The correspondence to zebrafish mutant phenotype is only authors' interpretation, and does not imply a genetic correspondence. This scheme is drawn merely to provide the readers with an overview of mutant phenotypes, and the details are not necessarily precise.

often is a reflection of earlier patterning defects. For instance, the *baltan* mutant shows severe degeneration in the forebrain and has an early patterning defect (Kitagawa et al., 2004).

2.4.2. Early PGC mutants

Many mutations affecting the distribution and/or abundance of PGCs at st. 26 were identified (Sasado et al., 2004). Mutations in 10 genes caused an altered distribution of PGCs, affecting PGC migration, accumulation and redistribution. The majority of mutant phenotypes in this class were associated with other morphological abnormalities, suggesting that the mutated gene is involved in various aspects of organogenesis. All of the mutations that reduced the number of PGCs exerted their effects only when the mother was a heterozygous carrier, indicating the contribution of maternal factors to the determination of PGC abundance.

2.4.3. Later-stage germ cell mutants

Screening of germ cells for *vasa* expression was also carried out at the larval stage when the sex of an animal can be distinguished by the abundance of *vasa*-positive germ cells. The female gonad is large and asymmetric and the male gonad is smaller and symmetric, as shown in Fig. 3.

The proliferation and/or distribution of germ cells during gonadal development was affected in mutants corresponding to 13 genes (Morinaga et al., 2004). Three mutations caused an increase in the number of germ cells. One interesting mutation, *totoro*, caused the tumorous growth of immature germ cells in homozygous juvenile adults. In other mutants, the abnormal distribution of germ cell clusters was accompanied by an irregular gonad shape, suggesting an interaction between germ cells and non-germ line gonadal anlage in gonadal development.

2.4.4. Lateral line mutants

The lateral line system is a sensory organ found in fish and amphibians. The posterior lateral line nerve (PLLn) shows stereotyped projections from the hindbrain to the neuromasts, groups of cells receiving sensory stimuli in the trunk. Mutations in four genes were isolated that affected the PLLn trajectory. Among the mutations identified, *kazura* (*kaz*) and *yanagi* (*yan*) mutations displayed specific defects in projection of the posterior lateral line nerve. The *yan* and *kaz* mutants also exhibited defects in the migration of primordial germ cells.

2.4.5. Mutants affecting liver development and function

Mutations in 19 genes affected the liver at various stages of development (Watanabe et al., 2004). These mutations were classified into five phenotypic groups in terms of liver morphogenesis, laterality, bile color, lipid metabolism and endoderm formation. Mutations in the first group, *kakurenbo*, *hiogi*, and *origami*, affect the size of the liver as well as the morphology of the gall bladder and gut, suggesting that these genes are involved in gut endoderm development.

2.4.6. Thymus mutants

Cells derived from three germ layers, neural crest cells from the ectoderm, lymphocytes from the mesoderm and cells of the thymic anlage from the endodermal pharyngeal pouch are thought to contribute to thymus organogenesis (Manley, 2000; Jenkinson et al., 2003; Bennett et al., 2002; Gill et al., 2002). Using *rag1* (*recombination activating gene 1*) expression in thymocytes as a marker of thymus development, we isolated 24 mutations defining at least 13 genes (Iwanami et al., 2004). Several mutants showed a range of defects in the pharyngeal arches from which the thymus anlagen develops. Thus, the primary defect may reside in the thymus anlage, leading to the failure of thymus formation. Other mutants with defective *rag1* expression showed normal pharyngeal arch development, suggesting that the mutations disrupt colonizing lymphocytes.

2.4.7. Eye mutants

The Kyoto screen together with previous morphological screens identified 60 mutations that affect retinal development (Loosli et al., 2004). The mutants were grouped into five classes: 11 mutants were affected in neural plate and optic vesicle formation, 15 mutants showed impaired growth of optic vesicles, 18 mutants were defective in optic cup development, 13 mutants showed abnormal retinal differentiation, 12 of which had small eyes and one caused enlarged eyes, and three mutants had abnormal retinal pigmentation.

2.4.8. Retino-tectal mutants

In Medaka, as in other lower vertebrates, the axons of RGCs project to the visual center of the brain, the optic tectum. To project the image on the retina precisely, all the RGC axons connect to the opposite side (contralateral) of the tectum, preserving the topological relationship with different points on the retina. Mutations in five genes affecting the projections of RGC axons to the retina were identified (Yoda et al., 2004). The misrouting of RGC axons occurred either between the retina and chiasm (Group 1 mutants) or between the chiasm and the tectum (Group 2 mutants). While misrouted axons reached the tectum on the same side (ipsilateral) of the retina in Group 1 mutants, misrouted axons did not project to the tectum in Group 2 mutants. Defects appear to be restricted to RGC axons in contrast to previously described zebrafish mutants (Karlstrom et al., 1996), as other tissues appear unaffected in the Medaka mutants.

2.4.9. Somitogenesis mutants

Mutations in nine genes affected somite formation and mutants were classified into two groups (Elmasri et al., 2004). Group 1 mutations caused phenotypes characterized by the complete or partial absence of somites or somite boundaries and Group 2 mutations resulted in fused somites or somites of irregular size and shape. The majority of

the mutants exhibited somitic phenotypes, such as individually fused somites and irregular somite sizes, that were distinct from those found in zebrafish (van Eeden et al., 1996). Three mutations were also isolated that produced characteristic phenotypes similar to those of zebrafish mutations affecting the Delta/Notch signaling pathway (van Eeden et al., 1996).

2.4.10. γ-Ray sensitivity mutants

A new type of screen was modified for fish to recover mutants that exhibit increased sensitivity to γ-ray radiation during development (Aizawa et al., 2004). After irradiation of F3 embryos using a dose at which wild-type embryos readily recover from damage, mutants were obtained by screening for whole-embryo viability. Three genes termed *ric* (radiation-induced curly tailed) *1–3* were identified in this screen. The *ric1* mutation was found to affect the repair of double-stranded DNA breaks induced by γ-ray, suggesting a DNA surveillance function for the *ric1* gene product during early embryogenesis (Aizawa et al., 2004).

3. Discussion

We have summarized the characteristics of developmental mutants collected in the first large-scale systematic screen carried out in Medaka in which multiple phenotypic traits were assayed. We observed much commonality between Medaka and zebrafish mutants, as may be expected, but also significant differences in the phenotypic spectrum between the two fish species. This finding validates the use of two complementary fish model systems for mutational analyses to probe developmental and cellular processes.

From a practical point of view, the visibility of a particular tissue during inspection of an embryo is an important factor in determining the ease of mutant identification. In a Medaka embryo, internal organs such as the liver and gall bladder are more conspicuous than those in zebrafish, while the notochord and melanophores are not as easily assayed. The types of mutants isolated in zebrafish and Medaka screens indeed reflect this difference in ease of tissue visualization (Haffter et al., 1996; Driever et al., 1996).

3.1. Distinct phenotypes between Medaka and zebrafish

The similarity in embryogenesis between Medaka and zebrafish allows the comparison and correspondence of developmental stages, morphogenetic landmarks, and hence mutant phenotypes. An important observation is that mutations in Medaka cause unique phenotypes that have so far not been described for zebrafish. For example, many Medaka mutations that affect forebrain development cause novel phenotypes that do not have an obvious correspondence to those of zebrafish mutants (Kitagawa et al., 2004).

The extent and timing of functional overlap among related genes may be sufficiently different to produce different sets of mutant phenotypes between the two fish models. Alternatively, regulation of forebrain development may involve divergent genetic pathways in the two species. Another formal possibility is that the susceptibility of some genetic loci to mutagenesis is substantially different between Medaka and zebrafish. In any event, the distinct phenotypes of the recovered mutants underscore the value of studying Medaka and zebrafish in parallel.

3.2. Phenotypes shared by Medaka and zebrafish mutants

Several Medaka mutants show a high degree of phenotypic similarity to zebrafish mutants. Recovered mutants with specific defects (Kitagawa et al., 2004; Watanabe et al., 2004) exhibited phenotypes resembling those of zebrafish *bozozok*, *one-eyed-pinhead*, *cyclops*, *masterblind*, *no isthmus*, *acerebellar*, *no tail* and *spadetail* mutants (Haffter et al., 1996; Driever et al., 1996).

A shared phenotype does not necessarily indicate that exactly the same set of genes or signals operate in the two fishes. Thus, even when the mutant phenotype is very similar, the identification of causal genes in both species is of great interest in understanding the genetic mechanisms involved in a given developmental process. Of particular interest are the cases in which different numbers of genes are assigned to the same phenotypic groups. In zebrafish, single genetic loci are responsible for the phenotypes of *one-eye-pinhead* (Schier et al., 1996) and *parachute* mutants (Jiang et al., 1996), but in Medaka, mutations in three genes give rise to phenotypes that are analogous to each zebrafish gene (Kitagawa et al., 2004).

Another interest would be to learn how the mutational disruption of orthologous genes results in different phenotypes in the two species. This will reveal how genetic mechanisms in the genesis of an organ can vary, and how the usage and/or regulation of orthologous genes has diversified in phylogeny. Differences in expression patterns and mutant phenotypes of orthologous genes in two related species have been discussed in terms of a model of gene duplication and complementing degenerative mutations (Force et al., 1999).

3.3. Mutations affecting tissue organization

Mutants with abnormalities in tissue organization and integrity fell into three distinct phenotypic groups. The first two groups appear to be unique to Medaka. In the first group of mutants, the initial specification of various brain regions appears to proceed normally, but these regions are gradually dislocated and/or disorganized by later stages of development. This was observed for the *fukuwarai*, *yuzen* and *kagome* mutants (Kitagawa et al., 2004; Watanabe et al., 2004). The second group, represented by *hirame*, is defective in the convergent movements of subsets of cells

toward the dorsal axis. While epiblast cells appear to converge normally in this mutant, cellular convergence in the hypoblast is seriously impaired, resulting in a reduced dorso-ventral thickness of the tissue along the body axis (Watanabe et al., 2004). By contrast, in zebrafish *silberblick* (Heisenberg et al., 2000), *knypek* (Topczewski et al., 2001) and *trilobite* mutants (Jessen et al., 2002), medial convergence of cells in both the epiblast and hypoblast layers is affected. In *spadetail* zebrafish mutants, the convergence of paraxial and intermediate mesoderm fails in the trunk region while epiblast movements are relatively normal. The last group consists of the *oobesshimi*, *samidare* and *shigure* mutants that are characterized by the exfoliation of neural cells in the ventricle (Kitagawa et al., 2004), reminiscent of zebrafish *parachute* mutants (Erdmann et al., 2003; Lele et al., 2002).

3.4. Development of primordial germ cells and the lateral line

The early development of primordial germ cell (PGC) is considerably different between Medaka and zebrafish. In zebrafish, germplasm-derived *vasa* mRNA is localized close to the cleavage plane at the four-cell stage, and this is reflected by four-cell clusters with high *vasa* expression close to the blastoderm margin at the onset of gastrulation (Weidinger et al., 1999). In Medaka, *vasa*-expressing cells appear only at the late-gastrula stage, and are scattered in the posterior one-third of the embryonic shield (Shinomiya et al., 2000). These observations are consistent with the report that fish of the ostariophysan clade (which includes zebrafish) localize *vasa* mRNA to the germplasm, and those of the euteleost clade (which includes Medaka) do not (Knaut et al., 2002). The subsequent migration of PGCs to the gonadal anlage has some similarity between the two species, although the pathways of cellular migration differ (Sasado et al., 2004). Medaka mutations affecting PGC development were screened for altered vasa expression, and mutations in 10 genes that affect PGC migration were identified (Sasado et al., 2004). Among the mutants, those of *kazura* and *yanagi* also have a defect in the distribution of lateral line primordia (Yasuoka et al., 2004).

In zebrafish, chemokine SDF1 and its G-protein-coupled receptor CXCR4b were shown to be required for the proper guidance of the migration of PGCs and lateral line primordia (Doitsidou et al., 2002; David et al., 2002). Indeed, a zebrafish mutant showing aberrant migration of PGCs and the lateral line has been isolated, and was recently found to have a mutation in the *cxcr4b* gene (Knaut et al., 2003).

The phenotypes of *kazura* and *yanagi* mutants with affected migration of PGCs and lateral line primordia resemble those of the zebrafish mutants in which SDF1/CXCR4b interaction is impaired (Yasuoka et al., 2004). While the *kazura* locus is linked to Medaka *cxcr4*, *yanagi* is neither linked to *cxcr4* nor *sdf1*, implying that *yanagi* codes for a new component of the SDF1-CXCR4b signaling pathway. In mice, it was also reported that germ cell migration and survival require SDF1/CXCR4 interaction (Molyneaux et al., 2003), indicating a high degree of evolutionary conservation in the mechanism regulating PGC migration.

vasa Expression was also employed to mark germ cells in developing gonad, and was useful in identifying gonad development mutants (Morinaga et al., 2004). In normal Medaka growth, distribution and differentiation of germ cells are clearly dimorphic reflecting genetically defined sex (Aida, 1921), but some gonad mutants lack this dimorphism, suggesting uncoupling of the gonadogenesis from the process downstream of the sex determination gene DMY (Matsuda et al., 2002; Nanda et al., 2002). Other mutants show abnormal *ftz-f1* expression that marks gonadal somatic cells. These mutants should prove useful in identifying the possible interaction of somatic and germ cells and the mechanisms underlying sexually dimorphic gonad development.

3.5. Prospect: towards elucidating vertebrate genome function

The analysis of mutational defects at the cellular level and the characterization of mutated genes are essential in defining the functions of genes in organogenesis and development. Focusing on neurogenesis, we have carried out cell lineage and migration analyses to map cell fates in Medaka (Hirose et al., 2004). A battery of genomic tools and resources for mutation mapping and gene cloning is already available (Zadeh Khorasani et al., 2004). The relatively small size of the Medaka genome, the availability of inbred strains with a high frequency of polymorphisms in Medaka, and the substantial syntenic preservation of gene alignments between Medaka and Fugu will facilitate positional cloning of mutated genes. The recent success of cloning the *b* gene (Fukamachi et al., 2001), *eyeless* gene (Loosli et al., 2001) and sex determining gene DMY (Matsuda et al., 2002) are just a prelude to forthcoming achievements. Genome sequencing on the basis of Bac contigs (Zadeh Khorasani et al., 2004), and by the whole-genome shotgun approach should accelerate such efforts. The accomplishment of ongoing whole-genome sequencing in Medaka and zebrafish will greatly facilitate comparative functional genomics in both species.

Medaka and zebrafish can be reared and bred in the same aquarium system, and can be studied by similar experimental approaches. Their commonality as small rapidly developing fish, as well as their unique genetic traits make them useful as complementary experimental animals. As described in this article, their use as model vertebrates is obviously advantageous in understanding the genomic functions involved in embryogenesis.

4. Materials and methods

4.1. Fish strains and fish maintenance

The Cab and Heino strains were obtained from the Wittbrodt laboratory and the Kaga strain from the Shima laboratory. The Cab strain, originating from the southern population of Medaka (Loosli et al., 2000), is homozygous for the recessive mutation of b^l of the *B* locus, that results in amelanotic melanophores. The Kaga strain is a wild-type strain originating from the northern population and was used for genetic linkage analysis (Yasuoka et al., 2004). The Heino strain is homozygous for the albino locus and was used for a specific locus test (Shima and Shimada, 1988). To establish a subline suitable for a mutagenesis screen, we have carried out brother–sister mating of the Cab and Kaga strains for more than nine generations. Strains with reasonable fecundity and a very low background of embryonic abnormalities in the temperature range between 18 and 32 °C, (Kyoto-Cab (K-Cab) and Kyoto-Kaga (K-Kaga) were established.

To carry out a large-scale mutagenesis screening, we used a fish cultivating system (Aquatic Habitats) equipped with 120 racks that can hold approximately 6000 tanks. Fish cultivation water was prepared by adding Red Sea salts (0.03%) to reverse osmosis water. Fish water was circulated with 10% daily exchange to new water.

4.2. Mutagenesis and breeding

Fish were mutagenized using available protocols for zebrafish and Medaka with modifications (Solnica-Krezel et al., 1994; Mullins et al., 1994; Loosli et al., 2000). Males of the K-Cab strain were treated with a solution containing 3 mM *N*-ethyl-*N*-nitrosourea (ENU) in 10 mM sodium phosphate (pH 7.0) at 27 °C for 1 h three times at three-day intervals. Starting from four weeks after the last ENU treatment, mutagenized males (G0) were crossed with K-Cab females to generate an F1 progeny (Fig. 1). Ten G0 males were crossed with homozygous Heino albino females for a specific locus test. The test was performed after many F1 fish were produced by crossing the G0 males with wild type females, and a large fraction of mutagenized males died before the test was completed. Thus, not all mutagenized males were subjected to the specific locus test. The mutational frequencies of hitting the albino locus under the described conditions were in the range of 1/196–1/726 among groups of 10 males tested. A total of 1300 F2 families were raised and used for mutant screening.

4.3. Mutant screening

4.3.1. Egg collection and phenotype recording

Matings of six to seven sibling pairs were made for each F2 family, and clutches of 15–40 eggs were collected per day from a pair. Ten clutches of eggs obtained from a pair were grown at three different temperatures (18, 28 and 33 °C) and screened for developmental abnormalities. A dissection stereomicroscope (Leica, MZ12.5) was used for embryo inspection. Observed phenotypes were recorded by a digital camera (Fuji Film, HC-300 Z) at the site of screening, and digitally archived into a database (Henrich et al., 2004).

4.3.2. Screening using live embryos

Live embryos were morphologically inspected at the three developmental stages, st. 19–21 (27–34 hpf), st. 25–27 (50–58 hpf) and st. 32–35 (4 dpf). Fig. 2 shows normal embryos at stages chosen for mutant screening. Liver-associated lipid metabolism was assessed by the accumulation of fluorescent PED6 metabolite in the liver and gall bladder at st. 34 (Watanabe et al., 2004). The metabolism of hemoglobin into bilirubin was monitored by the color of bile in the gall bladder in live embryos at st. 34. Sensitivity to γ-ray was assessed in terms of recovery at st. 32 from irradiation at 9.1 Gy (gray, which is defined as absorption of 1 J/kg. The absorbed-dose rate was monitored by a radio-photoluminescent glass dosimeter and a Fricke dosimeter) at st. 24 (Aizawa et al., 2004).

4.3.3. Whole-mount staining of fixed embryos

In situ hybridization and immunostaining were carried out for detecting specific molecular markers. Eggs were dechorionated by incubation in a pronase solution at 5 mg/ml (Sigma) and a crude hatching enzyme preparation (an extract of embryos at the hatching period, Ishida, 1944) for 1 h each at 28 °C, fixed with 4% paraformaldehyde (PFA) at stages indicated. PGCs and germ cells were visualized by the hybridization of fixed embryos/larvae with the Medaka *vasa* probe (Shinomiya et al., 2000) at st. 29 and 15 dpf, respectively (Sasado et al., 2004; Morinaga et al., 2004). Thymocytes in the thymus were detected by in situ hybridization using Medaka *rag1* probe at st. 32 (Iwanami et al., 2004). Axons and cell bodies of cranial nerves were immunostained using the mixture of anti-acetylated tubulin and HNK-1 antibodies at st. 32 (Kitagawa et al., 2004). RGC axons projecting to the tectum were visualized by injecting lipophilic fluorescent dyes DiI and DiO into the diagonal positions of the retina of fixed embryos at 9 dpf (Baier et al., 1996; Yoda et al., 2004).

4.4. Recovery of mutations and complementation test

After screening, carrier F2 fish were crossed with K-Cab fish to generate an F3 generation family. Carrier F2 males were then sacrificed under anesthesia to collect sperms for frozen stocks. Mutations were recovered in the F3 generation by random mating within F3 families and the identified pairs were crossed with the Kaga strain to generate an F4 generation to be used in linkage analysis. Complementation tests were performed by crossing heterozygous carriers of different mutations that cause similar phenotypes.

Acknowledgements

We would like to thank Drs Robert Kelsh, Francisco Pelegri, Fredericus van Eeden and John Postlethwait for critical reading and comments on this manuscript. We also thank Dr Koji Okamoto for his scientific administration, Haruka Momose and Takahiro Negishi for carrying out complementation tests. This work was supported initially by the PRESTO grant from Japan Science and Technology Agency (JST) to M.F.-S. and by the ERATO grant from JST to H.K.

References

Aida, T., 1921. On the inheritance of color in a fresh-water fish, *Aplocheilus latipes* Temminck and Schlegel, with special reference to sex-linked inheritance. Genetics 6, 554–573.

Aizawa, K., Mitani, H., Kogure, N., Shimada, A., Hirose, Y., Sasado, T., et al., 2004. Identification of radiation-sensitive mutants in the Medaka, *Oryzias latipes*. Mech. Dev. 121, 895–902.

Amores, A., Force, A., Yan, Y.L., Joly, L., Amemiya, C., Fritz, A., et al., 1998. Zebrafish hox clusters and vertebrate genome evolution. Science 282, 1711–1714.

Baier, H., Klostermann, S., Trowe, T., Karlstrom, R.O., Nusslein-Volhard, C., Bonhoeffer, F., 1996. Genetic dissection of the retinotectal projection. Development 123, 415–425.

Bennett, A.R., Farley, A., Blair, N.F., Gordon, J., Sharp, L., Blackburn, C.C., 2002. Identification and characterization of thymic epithelial progenitor cells. Immunity 16, 803–814.

Brand, M., Heisenberg, C.P., Warga, R.M., Pelegri, F., Karlstrom, R.O., Beuchle, D., et al., 1996. Mutations affecting development of the midline and general body shape during zebrafish embryogenesis. Development 123, 129–142.

Brenner, S., 1974. The genetics of *Caenorhabditis elegans*. Genetics 77, 71–94.

David, N.B., Sapede, D., Saint-Etienne, L., Thisse, C., Thisse, B., Dambly-Chaudiere, C., et al., 2002. Molecular basis of cell migration in the fish lateral line: role of the chemokine receptor CXCR4 and of its ligand, SDF1. Proc. Natl Acad. Sci. USA 99, 16297–16302.

Doitsidou, M., Reichman-Fried, M., Stebler, J., Koprunner, M., Dorries, J., Meyer, D., et al., 2002. Guidance of primordial germ cell migration by the chemokine SDF-1. Cell 111, 647–659.

Driever, W., Solnica-Krezel, L., Schier, A.F., Neuhauss, S.C., Malicki, J., Stemple, D.L., et al., 1996. A genetic screen for mutations affecting embryogenesis in zebrafish. Development 123, 37–46.

van Eeden, F.J., Granato, M., Schach, U., Brand, M., Furutani-Seiki, M., Haffter, P., et al., 1996. Mutations affecting somite formation and patterning in the zebrafish, *Danio rerio*. Development 123, 153–164.

Elmasri, H., Winkler, C., Liedtke, D., Sasado, T., Morinaga, C., Suwa, H., et al., 2004. Mutations affecting somite formation in the Medaka (*Oryzias latipes*). Mech. Dev. 121, 659–671.

Erdmann, B., Kirsch, F.P., Rathjen, F.G., More, M.I., 2003. N-cadherin is essential for retinal lamination in the zebrafish. Dev. Dyn. 226, 570–577.

Farber, S.A., Pack, M., Ho, S.Y., Johnson, I.D., Wagner, D.S., Dosch, R., et al., 2001. Genetic analysis of digestive physiology using fluorescent phospholipid reporters. Science 292, 1385–1388.

Force, A., Lynch, M., Pickett, F.B., Amores, A., Yan, Y.L., Postlethwait, J., 1999. Preservation of duplicate genes by complementary, degenerative mutations. Genetics 151, 1531–1545.

Fukamachi, S., Shimada, A., Shima, A., 2001. Mutations in the gene encoding B, a novel transporter protein, reduce melanin content in medaka. Nat. Genet. 28, 381–385.

Furutani-Seiki, M., Jiang, Y.J., Brand, M., Heisenberg, C.P., Houart, C., Beuchle, D., et al., 1996. Neural degeneration mutants in the zebrafish, *Danio rerio*. Development 123, 229–239.

Gill, J., Malin, M., Hollander, G.A., Boyd, R., 2002. Generation of a complete thymic microenvironment by MTS24(+) thymic epithelial cells. Nat. Immunol. 3, 635–642.

Haffter, P., Granato, M., Brand, M., Mullins, M.C., Hammerschmidt, M., Kane, D.A., et al., 1996. The identification of genes with unique and essential functions in the development of the zebrafish, *Danio rerio*. Development 123, 1–36.

Heisenberg, C.P., Brand, M., Jiang, Y.J., Warga, R.M., Beuchle, D., van Eeden, F.J., et al., 1996. Genes involved in forebrain development in the zebrafish, *Danio rerio*. Development 123, 191–203.

Heisenberg, C.P., Tada, M., Rauch, G.J., Saude, L., Concha, M.L., Geisler, R., et al., 2000. Silberblick/Wnt11 mediates convergent extension movements during zebrafish gastrulation. Nature 405, 76–81.

Henrich, T., Ramialison, M., Segerdell, E., Westerfield, M., Furutani-Seiki, M., Wittbrodt, J., Kondoh, H., 2004. GSD: a genetic screen database. Mech. Dev. 121, 959–963.

Hirose, Y., Varga, Z.M., Kondoh, H., Furutani-Seiki, M., 2004. Single cell lineage and regionalization of cell populations during Medaka neurulation. Development, in press.

Hrabe de Angelis, M.H., Flaswinkel, H., Fuchs, H., Rathkolb, B., Soewarto, D., Marschall, S., et al., 2000. Genome-wide, large-scale production of mutant mice by ENU mutagenesis. Nat. Genet. 25, 444–447.

Hyodo-Taguchi, Y., 1983. Effects of UV irradiation on embryonic development of different inbred strains of the fish *Oryzias latipes*. J. Radiat. Res. (Tokyo) 24, 221–228.

Ishida, J., 1944. Hatching enzyme in the fresh-water teleost, *Oryzias latipes*. Annot. Zool. Japon. 22, 137–154.

Ishikawa, Y., 2000. Medakafish as a model system for vertebrate developmental genetics. Bioessays 22, 487–495.

Iwanami, N., Takahama, Y., Kunimatsu, S., Li, J., Takei, R., Ishikura, Y., et al., 2004. Mutations affecting thymus organogenesis in Medaka, *Oryzias latipes*. Mech. Dev. 121, 779–789.

Jessen, J.R., Topczewski, J., Bingham, S., Sepich, D.S., Marlow, F., Chandrasekhar, A., Solnica-Krezel, L., 2002. Zebrafish trilobite identifies new roles for Strabismus in gastrulation and neuronal movements. Nat. Cell Biol. 4, 610–615.

Jiang, Y.J., Brand, M., Heisenberg, C.P., Beuchle, D., Furutani-Seiki, M., Kelsh, R.N., et al., 1996. Mutations affecting neurogenesis and brain morphology in the zebrafish, *Danio rerio*. Development 123, 205–216.

Karlstrom, R.O., Trowe, T., Klostermann, S., Baier, H., Brand, M., Crawford, A.D., et al., 1996. Zebrafish mutations affecting retinotectal axon pathfinding. Development 123, 427–438.

Kimmel, C.B., 1989. Genetics and early development of zebrafish. Trends Genet. 5, 283–288.

Kitagawa, D., Watanabe, T., Saito, K., Asaka, S., Sasado, T., Morinaga, C., et al., 2004. Genetic dissection of the formation of the forebrain in Medaka, *Oryzias latipes*. Mech. Dev. 121, 673–685.

Knaut, H., Steinbeisser, H., Schwarz, H., Nusslein-Volhard, C., 2002. An evolutionary conserved region in the vasa 3′UTR targets RNA translation to the germ cells in the zebrafish. Curr. Biol. 12, 454–466.

Knaut, H., Werz, C., Geisler, R., Nusslein-Volhard, C., 2003. A zebrafish homologue of the chemokine receptor Cxcr4 is a germ-cell guidance receptor. Nature 421, 279–282.

Jenkinson, W.E., Jenkinson, E.J., Anderson, G., 2003. Differential requirement for mesenchyme in the proliferation and maturation of thymic epithelial progenitors. J. Exp. Med. 198, 325–332.

Lele, Z., Folchert, A., Concha, M., Rauch, G.J., Geisler, R., Rosa, F., et al., 2002. Parachute/n-cadherin is required for morphogenesis and maintained integrity of the zebrafish neural tube. Development 129, 3281–3294.

Loosli, F., Koster, R.W., Carl, M., Kuhnlein, R., Henrich, T., Mucke, M., et al., 2000. A genetic screen for mutations affecting embryonic development in medaka fish (*Oryzias latipes*). Mech. Dev. 97, 133–139.

Loosli, F., Del Bene, F., Quiring, R., Rembold, M., Martinez-Morales, J.-R., Carl, M., et al., 2004. Mutations affecting retina development in Medaka. Mech. Dev. 121, 703–714.

Manley, N.R., 2000. Thymus organogenesis and molecular mechanisms of thymic epithelial cell differentiation. Semin. Immunol. 12, 421–428.

Matsuda, M., Nagahama, Y., Shinomiya, A., Sato, T., Matsuda, C., Kobayashi, T., et al., 2002. DMY is a Y-specific DM-domain gene required for male development in the medaka fish. Nature 417, 559–563.

Mayer, U., Ruiz, R.A.T., Berleth, T., Misera, S., Jürgens, G., 1991. Mutations affecting body organization in the *Arabidopsis* embryo. Nature 353, 402–407.

Molyneaux, K.A., Zinszner, H., Kunwar, P.S., Schaible, K., Stebler, J., Sunshine, M.J., et al., 2003. The chemokine SDF1/CXCL12 and its receptor CXCR4 regulate mouse germ cell migration and survival. Development 130, 4279–4286.

Morinaga, C., Tomonaga, T., Sasado, T., Suwa, H., Niwa, K., Yasuoka, A., et al., 2004. Mutations affecting gonadal development in Medaka, *Oryzias latipes*. Mech. Dev. 121, 829–839.

Mullins, M.C., Hammerschmidt, M., Haffter, P., Nusslein-Volhard, C., 1994. Large-scale mutagenesis in the zebrafish: in search of genes controlling development in a vertebrate. Curr. Biol. 4, 189–202.

Nanda, I., Kondo, M., Hornung, U., Asakawa, S., Winkler, C., Shimizu, A., et al., 2002. A duplicated copy of DMRT1 in the sex-determining region of the Y chromosome of the medaka, *Oryzias latipes*. Proc. Natl Acad. Sci. USA 99, 11778–11783.

Naruse, K., Fukamachi, S., Mitani, H., Kondo, M., Matsuoka, T., Kondo, S., et al., 2000. A detailed linkage map of medaka, *Oryzias latipes*: comparative genomics and genome evolution. Genetics 154, 1773–1784.

Nolan, P.M., Peters, J., Strivens, M., Rogers, D., Hagan, J., Spurr, N., et al., 2000. A systematic, genome-wide, phenotype-driven mutagenesis programme for gene function studies in the mouse. Nat. Genet. 25, 440–443.

Nüsslein-Volhard, C., Wieschaus, E., 1980. Mutations affecting segment number and polarity in *Drosophila*. Nature 287, 795–801.

Ohno, S., 1970. Evolution by Gene Duplication, Springer, Heidelberg.

Russell, L.B., Montgomery, C.S., 1982. Supermutagenicity of ethylnitrosourea in the mouse spot test: comparisons with methylnitrosourea and ethylnitrosourethane. Mutat. Res. 92, 193–204.

Sasado, T., Morinaga, C., Niwa, K., Shinomiya, A., Yasuoka, A., Suwa, H., et al., 2004. Mutations affecting early distribution of primordial germ cells in Medaka (*Oryzias latipes*) embryo. Mech. Dev. 121, 817–828.

Schier, A.F., Neuhauss, S.C., Harvey, M., Malicki, J., Solnica, K.L., Stainier, D.Y., et al., 1996. Mutations affecting the development of the embryonic zebrafish brain. Development 123, 165–178.

Shima, A., Shimada, A., 1988. Induction of mutations in males of the fish *Oryzias latipes* at a specific locus after gamma-irradiation. Mutat. Res. 198, 93–98.

Shinomiya, A., Tanaka, M., Kobayashi, T., Nagahama, Y., Hamaguchi, S., 2000. The vasa-like gene, olvas, identifies the migration path of primordial germ cells during embryonic body formation stage in the medaka, *Oryzias latipes*. Dev. Growth Differ. 42, 317–326.

Solnica-Krezel, L., Schier, A.F., Driever, W., 1994. Efficient recovery of ENU-induced mutations from the zebrafish germline. Genetics 136, 1401–1420.

Topczewski, J., Sepich, D.S., Myers, D.C., Walker, C., Amores, A., Lele, Z., et al., 2001. The zebrafish glypican knypek controls cell polarity during gastrulation movements of convergent extension. Dev. Cell 1, 251–264.

Watanabe, T., Asaka, S., Kitagawa, D., Saito, K., Kurashige, R., Sasado, T., et al., 2004. Mutations affecting liver development and function in Medaka, *Oryzias latipes*, screened by multiple criteria. Mech. Dev. 121, 791–802.

Weidinger, G., Wolke, U., Koprunner, M., Klinger, M., Raz, E., 1999. Identification of tissues and patterning events required for distinct steps in early migration of zebrafish primordial germ cells. Development 126, 5295–5307.

Wittbrodt, J., Shima, A., Schartl, M., 2002. Medaka: a model organism from the far East. Nat. Rev. Genet. 3, 53–64.

Yamamoto, T.O., 1965. Estriol-induced XY females of the medaka (*Oryzias latipes*) and their progenies. Gen. Comp. Endocrinol. 5, 527–533.

Yasuoka, A., Hirose, Y., Yoda, H., Aihara, Y., Suwa, H., Niwa, K., et al., 2004. Mutations affecting the formation of posterior lateral line system in Medaka, *Oryzias latipes*. Mech. Dev. 121, 729–738.

Yoda, H., Hirose, Y., Yasuoka, A., Sasado, T., Morinaga, C., Deguchi, T., et al., 2004. Mutations affecting retinotectal axonal pathfinding in Medaka, *Oryzias latipes*. Mech. Dev. 121, 715–728.

Zadeh Khorasani, M., Hennig, S., Imre, G., Asakawa, S., Palczewski, S., Berger, A., et al., 2004. A first generation physical map of the medaka genome in BACs essential for positional cloning and clone-by-clone based genomic sequencing. Mech. Dev. 121, 903–913.

ELSEVIER

Mechanisms of Development 121 (2004) 673–685

www.elsevier.com/locate/modo

Research paper

Genetic dissection of the formation of the forebrain in Medaka, *Oryzias latipes*

Daiju Kitagawa[a], Tomomi Watanabe[a], Kota Saito[a], Satoshi Asaka[a], Takao Sasado[b], Chikako Morinaga[b], Hiroshi Suwa[b], Katsutoshi Niwa[b], Akihito Yasuoka[c], Tomonori Deguchi[d], Hiroki Yoda[d], Yukihiro Hirose[e], Thorsten Henrich[b], Norimasa Iwanami[f], Sanae Kunimatsu[f], Masakazu Osakada[g], Chritoph Winkler[h], Harun Elmasri[h], Joachim Wittbrodt[i], Felix Loosli[i], Rebecca Quiring[i], Matthias Carl[i], Clemens Grabher[i], Sylke Winkler[i], Filippo Del Bene[i], Akihiro Momoi[d], Toshiaki Katada[a], Hiroshi Nishina[a], Hisato Kondoh[b,d], Makoto Furutani-Seiki[b,*]

[a]*Department of Physiological Chemistry, Graduate School of Pharmaceutical Sciences, The University of Tokyo, Tokyo 113-0033, Japan*
[b]*Japan Science and Technology Agency, ERATO, Kondoh Differentiation Signaling Project, Kawaracho14, Yoshida, Sakyoku, Kyoto 606-8305, Japan*
[c]*Graduate School of Agricultural and Life Sciences, The University of Tokyo, Tokyo 113-0033, Japan*
[d]*Graduate School of Frontier Biosciences, Osaka University, Osaka, 565-0871, Japan*
[e]*Graduate School of Biostudies, Kyoto University, Kyoto 606-8502, Japan*
[f]*Division of Experimental Immunology, Institute for Genome Research, The University of Tokushima, Tokushima 770-8503, Japan*
[g]*Department of Molecular Medicine and Pathophysiology, Research Institute, Osaka Medical Center for Cancer and Cardiovascular Diseases, Osaka 537-8511, Japan*
[h]*Department of Physiological Chemistry I, Biocenter, University of Wuerzburg, Wuerzburg, Germany*
[i]*Developmental Biology Programme, EMBL, D-69117, Heidelberg, Germany*

Received 1 February 2004; received in revised form 16 March 2004; accepted 18 March 2004

Abstract

The forebrain, consisting of the telencephalon and diencephalon, is essential for processing sensory information. To genetically dissect formation of the forebrain in vertebrates, we carried out a systematic screen for mutations affecting morphogenesis of the forebrain in Medaka. Thirty-three mutations defining 25 genes affecting the morphological development of the forebrain were grouped into two classes. Class 1 mutants commonly showing a decrease in forebrain size, were further divided into subclasses 1A to 1D. Class 1A mutation (1 gene) caused an early defect evidenced by the lack of *bf1* expression, Class 1B mutations (6 genes) patterning defects revealed by the aberrant expression of regional marker genes, Class 1C mutation (1 gene) a defect in a later stage, and Class 1D (3 genes) a midline defect analogous to the zebrafish *one-eyed pinhead* mutation. Class 2 mutations caused morphological abnormalities in the forebrain without considerably affecting its size, Class 2A mutations (6 genes) caused abnormalities in the development of the ventricle, Class 2B mutations (2 genes) severely affected the anterior commissure, and Class 2C (6 genes) mutations resulted in a unique forebrain morphology. Many of these mutants showed the compromised *sonic hedgehog* expression in the zona-limitans-intrathalamica (zli), arguing for the importance of this structure as a secondary signaling center. These mutants should provide important clues to the elucidation of the molecular mechanisms underlying forebrain development, and shed new light on phylogenically conserved and divergent functions in the developmental process.

Keywords: Forebrain; Telencephalon; Diencephalon; Mutants; Medaka; Mutagenesis screen

1. Introduction

The vertebrate forebrain, consisting of the telencephalon and diencephalon, is formed at the most rostral portion of the developing central nervous system (CNS). The telencephalon is the highest-order processor of neural functions,

* Corresponding author. Tel./fax: +81-75-771-9362.
E-mail address: furutaniseiki@msi.biglobe.ne.jp (M. Furutani-Seiki).

0925-4773/$ - see front matter © 2004 Elsevier Ireland Ltd. All rights reserved.
doi:10.1016/j.mod.2004.03.010

and the diencephalon is the conduit for ascending sensory information. Each territory of the forebrain is further regionalized along the respective anteroposterior (AP) and dorsoventral (DV) axes. These structures in the forebrain and their connections are essential for processing sensory information, integrating of new sensory information with established memories, and then formulating and effecting behavioral responses (Wilson and Rubenstein, 2000; Rallu et al., 2002).

The vertebrate forebrain was proposed to be subdivided in a segment-like manner into transverse neuromeric domains (prosomeres) analogous to rhombomeres in the hindbrain; on the basis of restricted expression patterns of transcription factors (neuromeric model, Bulfone et al., 1993; Figdor and Stern, 1993; Puelles and Rubenstein, 1993; Hauptmann and Gerster, 2000).

In all vertebrates, the developing telencephalon is subdivided into the dorsal (pallial region, expressing *emx1*) and ventral (subpallial region, expressing *dlx2*) domains. In the mammalian telencephalon, dorsal, pallial regions give rise to the cortex, while ventral, subpallial regions give rise to the basal ganglia. Similar pallial and subpallial subdivisions of the telencephalon exist in all vertebrates (Fernandez et al., 1998; Puelles et al., 2000), although the adult derivatives of these subdivisions vary among species.

The diencephalon is proposed to be divided into four longitudinal neuronal zones—dorsally, epithalamus, dorsal thalamus, ventral thalamus; and ventrally, hypothalamus (Figdor and Stern, 1993; Hauptmann et al., 2002). The dorsal and ventral thalami are divided by the zona limitans intrathalamica (zli). Although it is yet to be proven, the zli has been suggested to be a secondary signaling center, since the secreted signaling protein *sonic hedgehog* (*shh*) is expressed in the zli.

Theories of the formation of the subdivisions of the forebrain, however, are established on the bases of restricted expression patterns, mostly of transcription factors. Most of these transcription factors were cloned either by the homology of genes identified in the forward genetic mutant screening of invertebrates, such as *Drosophila melanogaster* and *Caenorhabditis elegans*, or by expression pattern screening. Functional studies of these genes have been carried out by the reverse genetic approach in the mouse or gain-of-function studies in chick, *Xenopus* and zebrafish. These studies, however, were still limited to the genes initially cloned by homology or expression patterns, but not their functions.

Genome-wide forward genetic screening based on the functions of genes, carried out using zebrafish for the first time in vertebrates, together with gene knock-out mice, established a genetic basis for the three key signaling pathways for the patterning of the forebrain. The Nodal pathway acts upstream of Shh signaling to specify the ventral telencephalon (Rohr et al., 2001; Varga et al., 2001), but Nodal and Shh signaling have distinct and cooperative roles in the development of the ventral diencephalon (Mathieu et al., 2002). However, the precise roles of Shh signaling, such as the source and time of action for the patterning the forebrain, remain to be elucidated. Wnt signaling is also reported to be important for patterning of the forebrain along the anteroposterior (A–P) axis (Kim et al., 2000; Heisenberg et al., 2001). The first row of cells at the rostral margin of the neural plate were shown to pattern the anterior forebrain anteroposteriorly (Houart et al., 1998) and its function has been ascribed to the secretion of the Wnt antagonist, *tlc* (Houart et al., 2002), corroborating the importance of Wnt signaling for A–P patterning in the forebrain in zebrafish. Nevertheless, insights obtained from existing mutants are still fragmentary due to the limited number of mutants.

In vertebrates in which the functions of multiple genes often overlap, mutagenesis screens in a single species is not sufficient for uncovering all functioning genes in a genetic cascade or in the development of an organ, but this limitation should be largely alleviated by the use of another related animal species. Thus, to define the genetic components of the signaling required for patterning of the forebrain and their interplay, we have undertaken a large-scale mutagenesis screen in Medaka. Here, we report the initial characterization of 33 mutations in 25 complementation groups exhibiting specific defects in the development of the forebrain. These mutants show a reduction in the size of the telencephalon, and defects in the formation of the ventricle or axogenesis. These mutants are often phenotypically distinct from those of mutants isolated in zebrafish (Brand et al., 1996a,b; Furutani-Seiki et al., 1996; Heisenberg et al., 1996; Schier et al., 1996), supporting the importance of this fish species which complements zebrafish.

2. Results

2.1. Development and regionalization of forebrain in wild-type Medaka embryos

The forebrain formed at the most rostral portion of the neural plate is composed of the telencephalon and diencephalon, occupying its dorsoanterior and ventroposterior portions, respectively. In Medaka, the forebrain becomes distinguishable from the midbrain at the histological level at stage 19 (st. 19), 27 hours post fertilization (hpf) at 28 °C (Fig. 1A), (Iwamatsu, 1994), and morphologically at st. 21 (Fig. 1B). During st. 19 and 21, the tissue initially located at the rostral end of the brain tissue is displaced to the ventral side of the brain. At st. 23 (41 hpf), the forebrain ventricle starts to form (Fig. 1C). During st. 23 and st. 27, the initially linear anteroposterior (A–P) axis through the brain is bent in the diencephalon area forming the ventral diencephalon (hypothalamus) overlain by both the dorsal diencephalon and mesensephalon, thereby

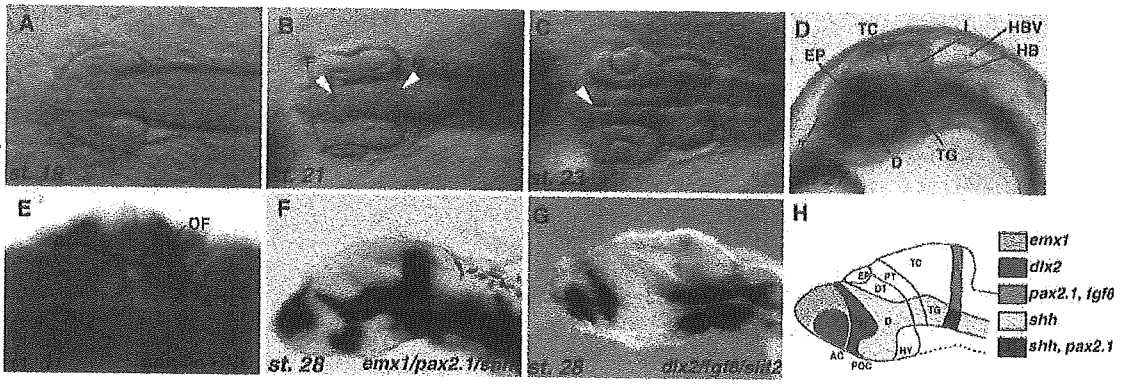

Fig. 1. Development and regionalization of the forebrain in wild-type Medaka embryos. (A–D) Morphology of the brain in Medaka live embryos. Dorsal view of wild-type embryo at (A) st. 19, (B) st. 21, (C) st. 23, (D) lateral view of the embryo at st. 27. (E) Major axonal scaffolds in the forebrain. Whole-mount immunostaining with anti-acetylated-tubulin and anti-HNK antibodies at st. 31. Ventral view of anterior portion of the head. (F,G) Whole-mount in situ hybridization analysis at st. 28. (F) *emx1*, *pax2.1*, *shh*; and (G) *dlx2*, *fgf8*, *slit2* as probes. (H) Schematic representation of gene expression patterns in subdivisions of the forebrain and midbrain. AC, anterior commissure; D, diencephalon; DT, dorsal thalamus; EP, epiphysis; F, forebrain; FV, forebrain ventricle; HB, hindbrain; HBV, hindbrain ventricle; HY, hypothalamus; I, isthmus; M, midbrain; OF, olfactory nerve; ON, optic nerve; POC, post-optic commissure; PT, pretectum; SOT, supraoptic tract; T, telencephalon; TC, tectum; TG, tegmentum; VT, ventral thalamus.

establishing the dorsoventral axis of the diencephalon (Fig. 1D). The cell layer of the roof of the telencephalon loses their thickness, and the telencephalon assumes its characteristic morphology. During st. 28–34 (64–131 hpf), cells proliferate extensively in the ventricular zone, and the ventricle loses its space (Ishikawa and Hyodo-Taguchi, 1994). The major axonal scaffolds in the forebrain, including commissural neurons, the supraoptic tract and sensory nerves, are formed by st. 34 (Fig. 1E).

In zebrafish, it was demonstrated that the expression patterns of marker genes define the transverse and longitudinal subdivisions within the forebrain and midbrain (Macdonald et al., 1994; Hauptmann and Gerster, 2000). Expression patterns of these markers seem to be well conserved in Medaka (Fig. 1F–H). For the initial characterization of Medaka forebrain mutants, we carried out whole-mount in situ hybridization analysis using a mixture of probes, *emx1/pax2.1/shh* and *dlx2/fgf8/slit2*. The dorsal and ventral telencephalon express *emx1* and *dlx2*, respectively. The diencephalon is divided into four domains; dorsal and ventral thalami, pretectum and hypothalamus. The zona limitans intrathalamica (zli), which expresses *shh*, divides the dorsal and ventral thalami. The ventral thalamus is marked by *dlx2* expression.

2.2. Identification of forebrain mutants in Medaka

Since a specific patterning defect often causes later occurrence of localized cell degeneration (Furutani-Seiki et al., 1996), we paid special attention to morphological abnormalities accompanied by cell degeneration. In the large-scale mutagenesis screen for embryonic pattern formation, we identified 33 mutations affecting forebrain development in Medaka mutants, exhibiting a variety of morphological defects and/or abnormal axonal pathways. These mutations were assigned to 25 complementation groups (Table 1). We classified these mutations into two groups, on the basis of the type of defects in the telencephalon. Class 1 mutations were those primarily affecting the size of the telencephalon, while Class 2 mutations were those mainly causing abnormalities in the forebrain shape without significantly affecting the size of the telencephalon. All the isolated mutations were zygotic recessive, and in this paper homozygous embryos are referred to as mutants. Two mutations turned out to be temperature sensitive; *kar*$^{i50\text{-}4A}$, which is sensitive to a low temperature (18 °C); and *ika*$^{j94\text{-}8A}$, which is sensitive to a high temperature (33 °C).

2.3. Class 1 mutations affecting telencephalon size

We have identified 15 mutations in 11 genes of this class causing reduction in telencephalon size (Fig. 2, arrowheads in A–F). According to the onset of the phenotype, we classified the Class 1 mutations into four subclasses, as summarized in Table 1.

2.3.1. Class 1A and 1B mutations affecting subregions of the telencephalon

In *kentoku* (*ket*$^{j23\text{-}3B}$) and *aonibi* (*aon*$^{j9\text{-}2F}$) mutant embryos, morphological defects appeared to be restricted to the telencephalon (Fig. 2B,C), whereas in *kobesshimi* (*kob*$^{j35\text{-}6D}$) and *bouzu* (*bou*$^{jr118\text{-}2A}$) mutant embryos, size reduction occurred also in the midbrain (Fig. 2D,E). On the other hand, *nopperabo* (*nop*$^{j80\text{-}19B}$) mutant embryos exhibited a characteristic phenotype, that is a reduction in forebrain size accompanied by the enlargement of the midbrain, reminiscent of that of *masterblind* (*mbl*) and *headless* (*hdl*) mutants in zebrafish (Fig. 2F).

Class 1 mutant embryos at st. 31 were immunochemically stained with anti-acetylated-tubulin and HNK1

Table 1
Mutations affecting formation of the forebrain

Gene	Symbol	Alleles	Forebrain phenotype	Other phenotypes
Class 1: mutations affecting the size of the telencephalon				
Class 1A: mutations affecting early specification of the telencephalon				
kentoku	*ket*	*j23-3B*	Telencephalon size reduced	
Class 1B: mutations affecting regionalization of the telencephalon				
aonibi	*aon*	*j9-2F, j60-3A*	Telencephalon size reduced	Lipid metabolism affected
kobesshimi	*kob*	*j9-10A, j35-6D, j54-3A*	Telencephalon size reduced	Midbrain slightly reduced
bouzu	*bou*	*jr118-2A*	Telencephalon size reduced	Midbrain anteroposteriorly reduced
nopperabo	*nop*	*j80-19B*	Telencephalon size reduced	Eyes missing, midbrain expanded
kumasaka	*kum*	*j54-20A*	Telencephalon size reduced	
usobuki	*uso*	*j14-26A*	Telencephalon size reduced	
Class 1C: a mutation affecting maintenance of the telencephalon				
hannya	*han*	*j41-3B*	Late telencephalon defect	–
Class 1D: mutations affecting formation of the midline neural tissue				
akatsuki	*aku*	*j22-15A, jf121-1A*	Telencephalon size reduced	Similar to zebrafish *oep*
akebono	*ake*	*j54-7A*	Telencephalon size reduced	Similar to zebrafish *oep*
mochizuki	*moc*	*j96-11B*	Telencephalon size reduced	Similar to zebrafish *oep*
Class 2: mutations affecting morphology of the telencephalon				
Class 2A: mutations affecting formation of the forebrain ventricle				
sarudahiko	*sar*	*j106-4A*	Forebrain ventricle reduced	Circulation, midline defect, tectum reduced
tengu	*ten*	*j2-11A, jr10-4D, j53-4C*	Forebrain ventricle reduced	Circulation, midline defect, tectum reduced
karuna	*kar*	*j50-4A*	Forebrain ventricle enlarged	Temperature sensitive at 18 °C
oobesshimi	*oob*	*j103-11A, j58-1A*	Forebrain ventricle enlarged	Tegmentum and hindbrain bumpy
samidare	*sam*	*j20-26A*	Forebrain ventricle enlarged	Similar to zebrafish *parachute* mutant
shigure	*sgu*	*j55-8A*	Forebrain ventricle enlarged	Similar to zebrafish *parachute* mutant
Class 2B: mutations affecting the formation of the anterior commissure				
ikazuchi	*ika*	*j94-8A*	Ectopic anterior commissure	Temperature sensitive at 33 °C, hindbrain bumpy
shikami	*shi*	*j92-3A*	Anterior commissure not formed	–
Class 2C: mutations causing forebrain dysmorphology				
baltan	*bal*	*j102-2A*	Forebrain dysmorphology, edema	Eyes small, tectum reduced, circulation defect, somite irregular
fukuwarai	*fuk*	*j8-33A, j93-4A*	Forebrain dysmorphology	Regions of CNS misplaced
yuzen	*yuz*	*j107-2D*	Forebrain dysmorphology	Regions of CNS misplaced
kagome	*kag*	*jr114-2D*	Forebrain dysmorphology	Regions of CNS misplaced
hirame	*hir*	*j54-20C*	Flattened, differentiation defect	CNS flat, heart beating next to ears
tobi	*tob*	*jr116-4A*	Protruding telencephalon	Eyes small

antibody to examine the paths and fasciculation of axons (Fig. 2G–L). In the wild type embryos, the olfactory nerve, anterior commissure, supraoptic tract and optic nerve were clearly stained (Fig. 2G). All Class 1 mutants showed interesting abnormalities in these nerves. In *ket* mutant embryos, anterior commissure nerves were not fully fasciculated (black arrowhead in Fig. 2H), displaced and lacked association with the olfactory nerve (white arrowheads in Fig. 2H), and the supraoptic tract was not clearly detected. In *aon* mutant embryos, the olfactory nerve and supraoptic tract were not detected, the anterior commissure lacked fasciculation (white arrowhead in Fig. 2I), and bundle formation of the optic nerve was also affected (black arrowhead in Fig. 2I). *kob* mutants were unique in that only olfactory nerve was affected and lacked fasciculation (arrowhead in Fig. 2J). In *bou* mutant embryos, the axons in the anterior commisure were totally defasciculated, and the commissure did not form (arrowhead in Fig. 2K). In the *nop* mutant embryos, all axonal paths were so severely affected and in astray that the nerves in the forebrain were not morphologically distinguishable each other (arrowhead in Fig. 2L). In addition, the olfactory bulbs appeared to be missing in *nop* mutant embryos (Fig. 2L). Thus, Class 1 mutants share the commonality of a reduced telencephalon size, but alterations of the nerves and their paths were affected distinctly.

Class 1 mutants were also examined for the regional markers of the forebrain by in situ hybridization with two sets of probes, *emx1/pax2.1/shh* and *dlx2/fgf8/slit2* (Fig. 2M–X). Consistent with a smaller telencephalon, Class 1 mutant embryos generally showed a reduction in *emx1* or *dlx2* expression in the telencephalon.

In *ket* and *nop* mutant embryos, the *emx1* expression was strongly reduced (black arrowhead in Fig. 2N,R) and

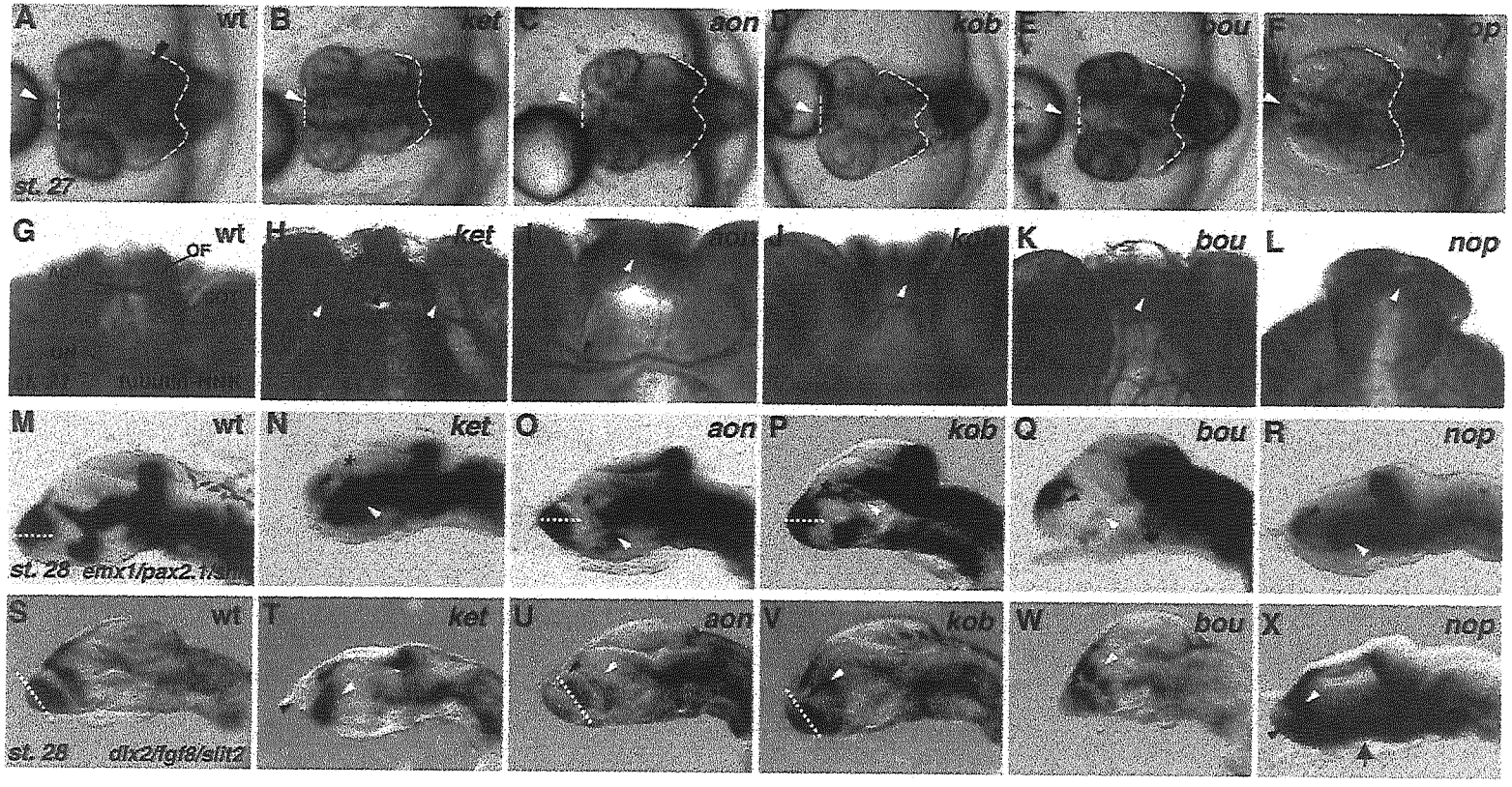

Fig. 2. Class 1 mutant phenotypes. (A,G,M,S) Wild type; (B,H,N,T) *ket*$^{j23\text{-}3B}$; (C,I,O,U) *aon*$^{j9\text{-}2F}$; (D,J,P,V) *kob*$^{j35\text{-}6D}$; (E,K,Q,W) *bou*$^{r118\text{-}2A}$; (F,L,R,X) *nop*$^{j80\text{-}19B}$ embryos. (A–F) Phenotypes of live Class 1 mutant embryos at st. 27 (dorsal view). White and black arrowheads indicate the positions of the telencephalon and midbrain, respectively. All Class 1 mutants show a reduction in the size of the telencephalon. Broken lines indicate the posterior edges of the telencephalon and the midbrain. (G–L) Whole-mount immuno-staining with anti-acetylated-tubulin and anti-HNK antibodies of embryos at st. 31. Ventral view of the anterior portion of the head. AC, anterior commissure; SOT, supraoptic tract; OF, olfactory nerve; ON, optic nerve. (M–X) In situ hybridization analysis of the forebrain of embryos at st 28. Lateral view of the head. (M–R) *emx1/pax2.1/shh*, and (S–X) *dlx2/fgf8/slit2* as probes, respectively.

the *dlx2* expression in the ventral telencephalon was almost absent (black arrowheads in Fig. 2T,X). In these mutants, the *shh* expression along the floor of the diencephalon (white arrowheads in Fig. 2N,R) dorsally expanded and, in *ket* mutant embryos, the expression in the zona limitans intrathalamica (zli) was lost (asterisk in Fig. 2N). The *dlx2* expression in the ventral thalamus showed an anterior shift (white arrowhead in Fig. 2T). In *nop* mutants, the *dlx2* expression marking the ventral thalamus anteriorly shifted, which was accompanied by the anterior expansion of the *dlx2* expression in the pharyngeal arch region (arrow in Fig. 2X).

In *aon* mutant embryos, the *emx1* expression shifted ventrally (broken line in Fig. 2M,O). Concomitantly, two domains of the *dlx2* expression in the ventral telencephalon and ventral thalamus shifted posteriorly (broken line in Fig. 2S,U to show the anterior limit of the *dlx2* expression; black and white arrowheads in Fig. 2U). The anteroventral region of the diencephalic *shh* expression was reduced (white arrowhead in Fig. 2O) and the *shh* expression in the zli was abolished (asterisk in Fig. 2O).

In *kob* mutants, the *emx1* expression shifted ventrally (broken line in Fig. 2P) and the *dlx2* expression in the ventral telencephalon shifted posteriorly (broken line and black arrowhead in Fig. 2V), and the *dlx2* expression in the ventral thalamus decreased (white arrowhead in Fig. 2V). *shh* expression in the zli and ventral diencephalon was low (asterisk and white arrowhead in Fig. 2P, respectively).

In *bou* mutant embryos, the *emx1* expression domain seems compressed anteroposteriorly (black arrowhead in Fig. 2Q) and the *dlx2* expression in the ventral thalamus became noncontinuous (white arrow head in Fig. 2W). The *shh* expression in the diencephalon was only rudimentary (white arrowhead in Fig. 2Q).

Thus, different patterning defects in the forebrain are included in these Class 1 mutants with smaller telencephalon. It is important to note that the majority of the mutants of this Class had an altered *shh* expression, particularly a reduction of *shh* expression in the zli.

2.3.2. Class 1A mutant kentoku representing an early fuction in telencephalon development

The expression of an early telencephalic marker *bf1* (Tao and Lai, 1992) was examined in all the Class 1 mutants. In wild-type Medaka embryos, *bf1* expression becomes detectable in the most anterior region of the brain at st. 19. *ket* mutant at st. 20 uniquely lacked the *bf1* expression (Fig. 3A,B). This observation indicated that *ket* is required in an early step in telencephalon development, possibly in the induction process. In *nop* mutant embryos, *bf1* expression was reduced at st. 20 probably due to the expansion of the diencephalon and mesencephalon at the expense of the telencephalon. In the rest of Class 1 mutants, *bf1* expression appeared normal (data not shown).

2.3.3. Class 1C mutation affecting maintenance of the telencephalon

In *hannya* ($han^{j41\text{-}3B}$) mutant embryos, the distance between the eyes decreased (arrow in Fig. 4A,E), but the floor plate was normal (data not shown), ruling out general midline defects. The expression of dorsal *emx1* was reduced in *han* mutant embryos (arrowheads in Fig. 4D,H). The projection pattern of trigeminal nerves was altered such that they did not extend toward the ventral surface of the forebrain at st. 31 (arrowheads in Fig. 4B,C,F,G). By contrast, the anterior commissure appeared normal. This phenotype was unique to *han* mutants and distinguished them from other Class 1 mutants.

2.3.4. Class 1D mutations exhibiting the phenotype similar to that of oep in zebrafish

The mutants of *akatsuki* ($aku^{j22\text{-}15A}$), *akebono*($ake^{j54\text{-}7A}$) and *mochizuki*($moc^{j96\text{-}11B}$), classified to 1D all displayed a drastic morphological phenotype similar to that of *one-eyed-pinhead* (*oep*) in zebrafish (Fig. 5A–D), where only one median eye was formed and the ventral brain tissue was severely affected. This phenotype was very similar to that of the zebrafish *oep* mutant (Schier et al., 1996). These three Medaka mutations sharing similar forebrain phenotypes complemented each other.

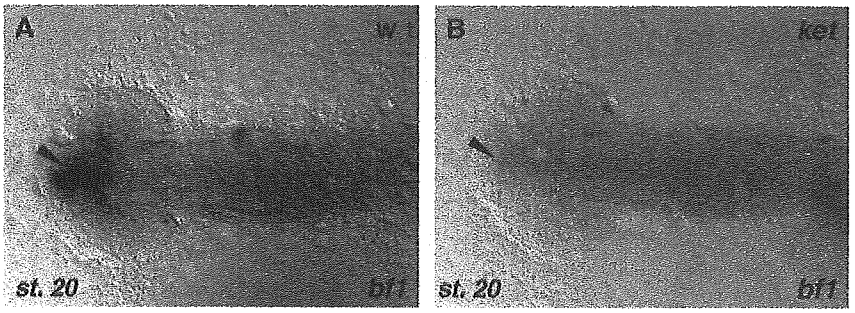

Fig. 3. Loss of *bf1* expression in $ket^{j23\text{-}3B}$ mutant embryo at st. 20. (A,B) Whole-mount in situ hybridization analysis of embryos at st. 20 with *bf1* probe. (A) Wild-type embryo. (B) *ket* mutant embryo.